



Technical Notes

Multiscale Optimization of Nanocomposites with Probabilistic Feature Descriptors

Pinar Acar*

Virginia Tech, Blacksburg, Virginia 24061

and

Veera Sundararaghavan[†] and Nicholas Fasanella[‡]

University of Michigan, Ann Arbor, Michigan 48109

DOI: 10.2514/1.J056791

Nomenclature

A	=	orientation distribution function
\bar{C}	=	averaged stiffness
\bar{E}_1	=	Young's modulus along axis 1
\bar{G}_{12}	=	shear modulus in 1–2 plane
\bar{k}	=	thermal conductivity coefficient
$\bar{\alpha}$	=	thermal expansion coefficient
$\bar{\alpha}_{\text{epoxy}}$	=	thermal expansion coefficient of epoxy
Φ_{epoxy}	=	epoxy volume fraction
Φ_{SWNT}	=	single-walled carbon nanotube volume fraction

I. Introduction

POLYMER-MATRIX composite materials are widely used in high-performance applications due to their high specific strength, high specific stiffness, fatigue resistance, and ease of manufacturing. Thermoset polymers are the most predominant type of matrix system, and epoxies specifically are preferred for aerospace-grade components due to their superior mechanical properties and resistance to environmental degradation due to moisture. Carbon nanotubes (CNTs) have been researched extensively due to their outstanding mechanical [1–3], electrical [4–6], and thermal properties [7,8]. Because of these exceptional properties and very high aspect ratios, forming CNT-polymer nanocomposites has become an attractive option to improve the properties of the polymer. This work particularly focuses on single-walled carbon nanotubes (SWNTs). SWNTs are an atom-thick single layer of graphene with a cylindrical structure and an elastic modulus around 1 TPa [9]. We have addressed a multiscale modeling and optimization methodology to further improve the structural and thermal performance of the SWNTs.

The interface between the CNT and epoxy plays an important role in the thermomechanical properties of nanocomposites. Experimental characterization of this interface is difficult, and thus molecular

modeling becomes an essential tool for relating molecular interfacial structure to bulk thermomechanical properties. Molecular dynamics (MD) was used previously to explore the effects on the mechanical and dilatometric properties by adding pristine and covalently functionalized SWNTs to cross-linked polymers [10,11]. MD allows for the effects of mechanical and thermal loading to be isolated and visualized in regions of interest where it may not be possible with experiments. MD, however, has well-known limitations regarding time and length scales; for example, the time step of an MD simulation is typically on the order of femtoseconds. It is defined by the fastest motion in the system, and vibrational frequencies are up to 3000 cm^{-1} , corresponding to the period on the order of 10 fs [12]. The limiting factor of the length scale is the number of atoms that can be included in the simulation, on the order of 10^3 – 10^8 atoms, leading to a simulation on the order of 10–100 nm [12]. To address these issues, a number of different multiscale approaches have been implemented by various researchers to model SWNT-polymer nanocomposites. Liu et al. used a multiscale approach, via MD and micromechanics, to study the effect of functionalization of CNTs on the damping characteristics of SWNT-polymer composites [13]. Seidel and Lagoudas calculated the effective elastic properties for CNT-reinforced composites through a variety of micromechanics techniques [14]. To accurately model the macroscopic behavior, many authors employ numerical techniques such as the finite element method (FEM). Li and Chou examined the effect of interfacial load transfer on the stress distribution, as well as the compressive behavior in CNT-polymer composites via a molecular structural mechanics model combined with FEM [15,16]. Namilae and Chandra also studied interfacial properties and developed a hierarchical multiscale methodology to link MD and FEM through atomically informed cohesive zone model parameters [17]. Spanos and Kontos developed a multiscale Monte Carlo and FEM for the effective elastic properties of SWNT-polymer nanocomposites [18]. Tserpes et al. used a multiscale representative volume element for modeling the tensile behavior of CNT-reinforced composites to integrate nanomechanics and continuum mechanics. [19]. Ionita used multiscale modeling via atomistic and mesoscale simulations to study SWNT-epoxy composites [20]. Yang et al. developed a sequential multiscale bridging model to characterize the CNT size effects and weakened bonding effects at the interface of CNT-polypropylene composites using MD and continuum micromechanics [21,22]. In many of the previous works, effects of preferential nanotube alignment are often modeled using expensive numerical (e.g., FEM) techniques.

In this work, we introduce a multiscale modeling technique that allows efficient control over the volume fraction and alignment of SWNTs. SWNT alignment in a composite is modeled using a compact representation of the orientation space while accounting for symmetry. The nanocomposite structure is represented using an orientation distribution function (ODF) that captures the volume density of different SWNT orientations. The averaged material properties, such as the stiffness elements, thermal conductivity, and thermal expansion, are calculated using the volume averaging equations that are linear in terms of the ODF values. Several studies focusing on the improvement/optimization of SWNT chemical and physical properties such as position, shape, linkage, morphology, flame synthesis, and spectroscopic properties are addressed in the literature [23–26]. However, the present study introduces a fully automated multiscale design optimization framework for the first time to identify the optimum nanotube alignments of SWNTs in different macroscale engineering problems. We first develop an optimization methodology using linear programming (LP) to calculate the optimal values of the ODFs to enhance the mechanical and thermal properties of the SWNT. The objective of the LP problem is defined as the maximization of the stiffness parameter, C_{11} . The design constraints are defined to ensure that the optimum design

Presented as Paper 2018-1157 at the 2018 AIAA/ASCE/AHS/ASC Structures, Structural Dynamics, and Materials Conference, Kissimmee, FL, 8–12 January 2018; received 6 October 2017; revision received 25 January 2018; accepted for publication 26 January 2018; published online 12 March 2018. Copyright © 2018 by Pinar Acar. Published by the American Institute of Aeronautics and Astronautics, Inc., with permission. All requests for copying and permission to reprint should be submitted to CCC at www.copyright.com; employ the ISSN 0001-1452 (print) or 1533-385X (online) to initiate your request. See also AIAA Rights and Permissions www.aiaa.org/randp.

*Assistant Professor, Department of Mechanical Engineering, Member AIAA.

[†]Associate Professor, Department of Aerospace Engineering, Member AIAA.

[‡]Department of Aerospace Engineering.

provides improvement in other stiffness parameters as well as the thermal conductivity and thermal expansion values in comparison with the randomly oriented nanotube alignment. In the next application, a cantilever beam problem is solved to minimize the thermal expansion, and the problem is constrained for vibration tuning. The sequential quadratic programming (SQP) is employed to find the optimum ODF values and satisfy the predefined vibration tuning constraints. The organization of the paper is as follows. Section II discusses the modeling of the material. Section III introduces the ODF approach to compute the properties of the nanocomposites. The optimization problem based on the LP approach is defined and the results are reported in Sec. IV. Section V addresses the SQP algorithm-based optimization for the thermal expansion problem. A summary of the paper with the potential future directions is given in Sec. VI.

II. Material Modeling

Diglycidyl ether of bisphenol A (DGEBA) is the epoxy chosen for this study. The curing agent used is diamino diphenyl sulfone (DDS). The epoxy molecules were cross-linked (cured) with 3-3' DDS. A major hurdle in creating accurate models for molecular simulation of industrial-grade epoxies is attaining realistic cross-linking densities, where a conversion percentage of 70%–95% is typically seen when measured through near-infrared (NIR) spectroscopy [27]. We use a method introduced by Christensen [28,29] to build epoxy networks using a “dendrimer” growth approach, which was previously presented by the authors [10,11].

The dendrimer growth approach was used to build the epoxy network in Materials Studio [30] containing 36 amine groups and 71 epoxy groups. An example representation of the dendrimer growth approach can be seen in Fig. 1. Simulations were performed under periodic boundary conditions, and the consistent valence force field (CVFF) [31] potential was used for bonded and nonbonded interactions in LAMMPS [32]. This force field has been used in previous studies to accurately predict thermodynamic properties of epoxy [33,34]. Of available epoxy sites, 75% were cross-linked, which is representative of many structural epoxies. To verify the accuracy of the initial dendrimer structure, the dilatometric curve simulated by MD was compared with experimental results, and the full elastic stiffness matrix was generated by conducting tensile and shear tests via MD to verify that the structure is isotropic. The thermal conductivity and elastic properties of these unit cells were reported in our previous publications [10,11].

To build the CNT/epoxy nanocomposites, a vacancy was created in the epoxy by moving atoms radially outward from a chosen point, and an single-walled armchair nanotube (4,4) was inserted in the space as shown in Fig. 2. Moving atoms caused many bonds to be displaced from their equilibrated length, and so the same annealing process ran previously via a sequence of conjugate gradient (CG) minimization and dynamics above and below glass transition temperature was used to minimize potential energy until the density converged. The methodology to add discontinuous CNTs is in a recent paper [35].

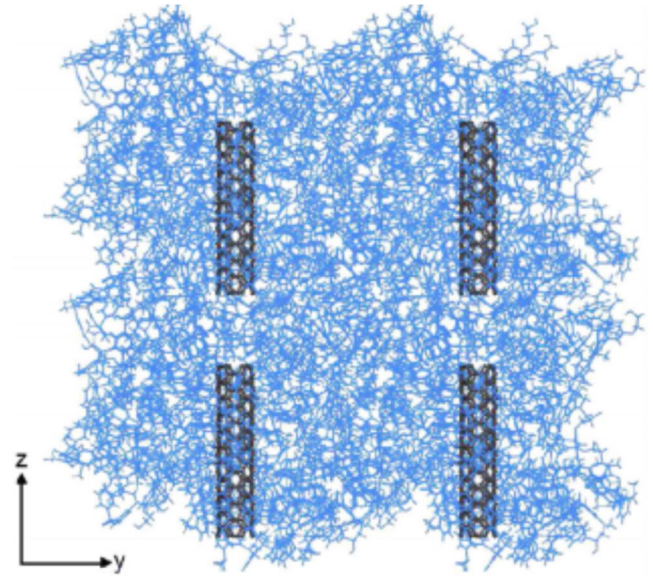


Fig. 2 Example nanotube spacing for discontinuous nanotubes that span 11/15 of the cell.

III. Modeling of Nanocomposites with the ODF Approach

MD has a well-known length scale restriction, with the dimension of each side of the MD lattice being limited to a few hundred angstroms. Thus, only a limited set of CNT volume fractions can be accessed using this approach. To achieve low CNT volume fractions that are representative of commercially available nanocomposites, excessively large unit cells need to be built. Instead, multiscale modeling based on the ODF approach is considered in this work. The ODF is a one-point probability function [36] and here it is used to describe the volume fractions of SWNTs as a function of orientation. The orientation (or alignment of the nanotube) is represented using an axis-angle format proposed by Rodrigues [37–39]. Here, the 3D rotation is based on the unique association of an orientation with an axis of rotation, \mathbf{n} , and a rotation angle, θ , about the axis. The details for the Rodrigues parameterization and ODF representation can be found in our earlier studies [40,41]. Because the SWNT-epoxy lattice is transversely isotropic and contains hexagonal symmetry, the 3D orientation space can be reduced to a small subset called the fundamental region that accounts for hexagonal symmetry.

Given the orientation-dependent property for an SWNT unit cell, $\chi(\mathbf{r})$, any equivalent macroscopic property can be expressed as a value or expectation value over the ODF given by

$$\bar{\chi} = \int_{\mathcal{R}} \chi(\mathbf{r}) A(\mathbf{r}, t) dv \quad (1)$$

The above equation is used to find the averaged values of the SWNT properties [42,43]. In this work, the upper-bound averaging is

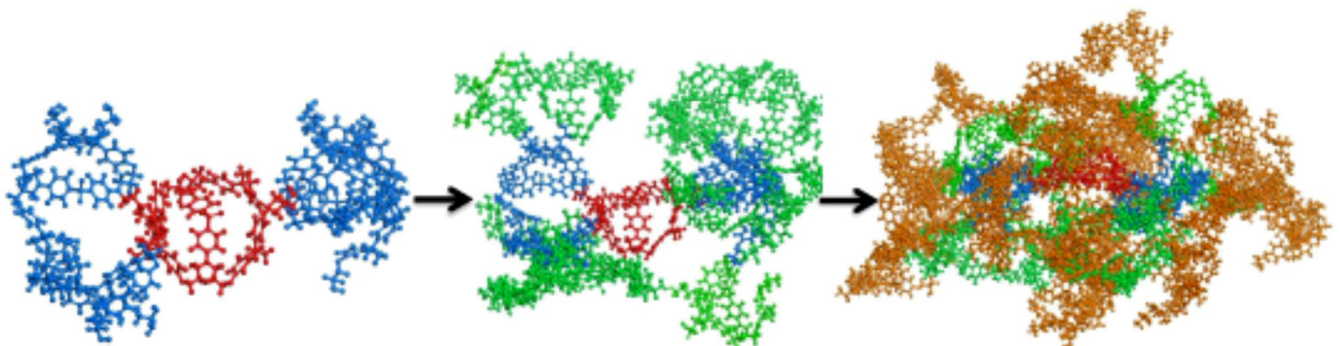


Fig. 1 Representation of dendrimer growth approach.

used to compute the stiffness, thermal expansion, and conductivity parameters, for example, $\bar{\chi}(\mathbf{r}) = \bar{C}_{ijkl}$, resulting in averaged stiffness \bar{C} . ODFs can be constructed to represent a fully random composite, fully aligned composite, and various percentages of aligned nanotubes. The orientation-dependent property obtained from Eq. (1) has the same volume fraction as the representative SWNT-epoxy lattice, which is the microscopic basis for the ODF. The volume fraction of SWNT is 3.7%, which is 7% by weight of unit cell. For numerical analysis, the fundamental region is discretized using a finite element mesh. The derivation of the property matrices with the finite element discretization is explained in details on our previous works [40,41]. The finite element discretization leads to a linear equation for the homogenization of the microstructural properties, such that $\bar{\chi} = \mathbf{p}^T \mathbf{A}$, where \mathbf{p} is the property matrix, and $\bar{\chi}$ is the averaged property of the SWNT. Different SWNT orientations are modeled with the finite element discretization in the Rodrigues orientation space, and each orientation is associated with a particular ODF value.

IV. Optimization of Nanotube Alignment Using Linear Programming

The orientation of the nanotubes can be controlled, which makes it possible to study the effects of nanotube alignment. The unit cell alignment of each element is assigned through the independent nodal point ODFs. The ODF representation is discretized using a FEM approach in Rodrigues fundamental region as shown in Fig. 3. These nodes are assigned weights based on the number of symmetric nodes and sampling volume in orientation space. The exact weight per node depends on how many equivalent nodes exist, and the volume weightage, \mathbf{q} , of the node in the normalization constraint. The randomly oriented design assumes that each orientation has the same volume fraction values. However, the material properties can be further improved by assigning different ODF values to different orientations. In the optimization applications the goal is to identify the optimal SWNT orientations given a fixed amount of epoxy (the SWNT volume fraction is always 3.7%). The first problem of interest here is to identify these optimal ODF values to optimize the averaged material properties by taking the advantage of the linear volume averaging equations with an LP solution. Some of the property matrices (\mathbf{p}^T) for the material properties (stiffness, thermal expansion, and conductivity) in the first problem are shown in terms of the single crystal values in Fig. 4.

The proposed optimization problem aims to maximize the value of the stiffness element, \bar{C}_{11} of the SWNT while assigning design constraints to ensure that the other design criteria (stiffness elements, thermal conductivity, and thermal expansion) should have enhanced values compared with a randomly oriented design. The thermal expansion and conductivity elements used in the applications are the (1,1) elements of the corresponding tensors. The optimization problem of interest is defined below:

$$\max \bar{C}_{11} \tag{2}$$

$$\text{subject to: } \bar{C}_{12}^{\text{opt}} \geq \bar{C}_{12}^{\text{random}} \tag{3}$$

$$\bar{\alpha}^{\text{opt}} \leq \bar{\alpha}^{\text{random}} \tag{4}$$

$$\bar{k}^{\text{opt}} \geq \bar{k}^{\text{random}} \tag{5}$$

$$\mathbf{q}^T \mathbf{A} = 1 \tag{6}$$

$$s = (A_i), \quad \text{where } i = 1, 2, \dots, 50 \tag{7}$$

where α shows the thermal expansion, and k shows the thermal conductivity. The superscripts opt and random denote the optimum and random designs. The optimization problem definition is modified according to a standard LP problem definition. The optimum results for the SWNT parameters provide an improvement in the objective function value as well as satisfying all the design constraints. These optimum results are given in Table 1 for all the design criteria in comparison with a random design. The optimum ODF design is also shown in Fig. 5.

V. Optimization of Nanotube Alignment for Thermal Expansion and Vibration Tuning

The next application is a nonlinear optimization problem for a cantilever beam. The objective of this optimization problem is to find the optimum ODF distribution of the SWNT that minimizes the thermal expansion coefficient of the beam while satisfying design constraints for natural frequencies. For this purpose the first bending and torsion natural frequencies of the beam are expected to vary in between some particular numerical values for vibration tuning.

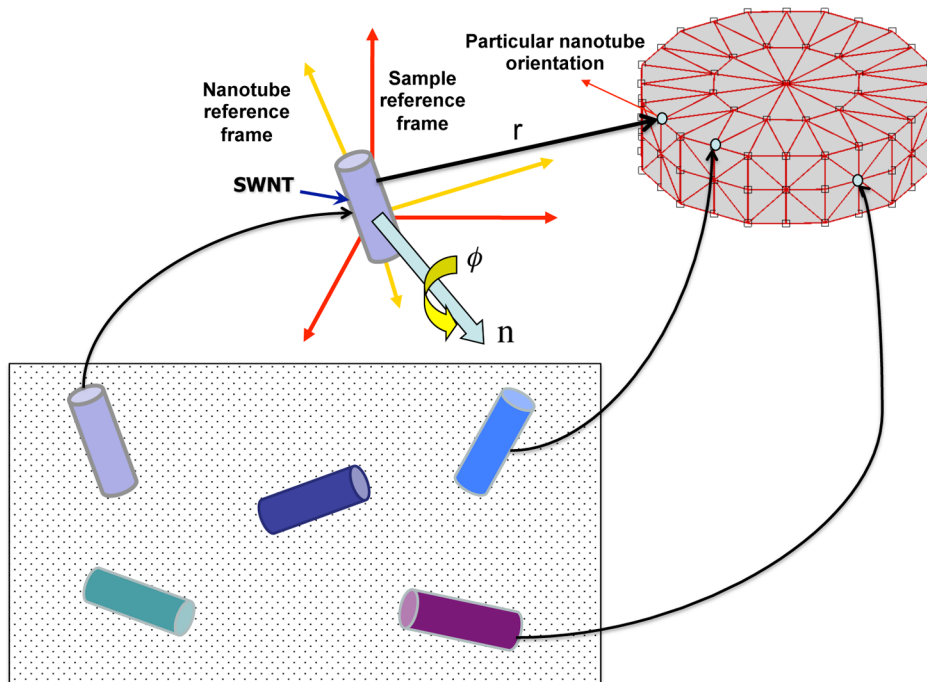


Fig. 3 ODF representation for SWNT in the Rodrigues fundamental region for hexagonal crystal symmetry.

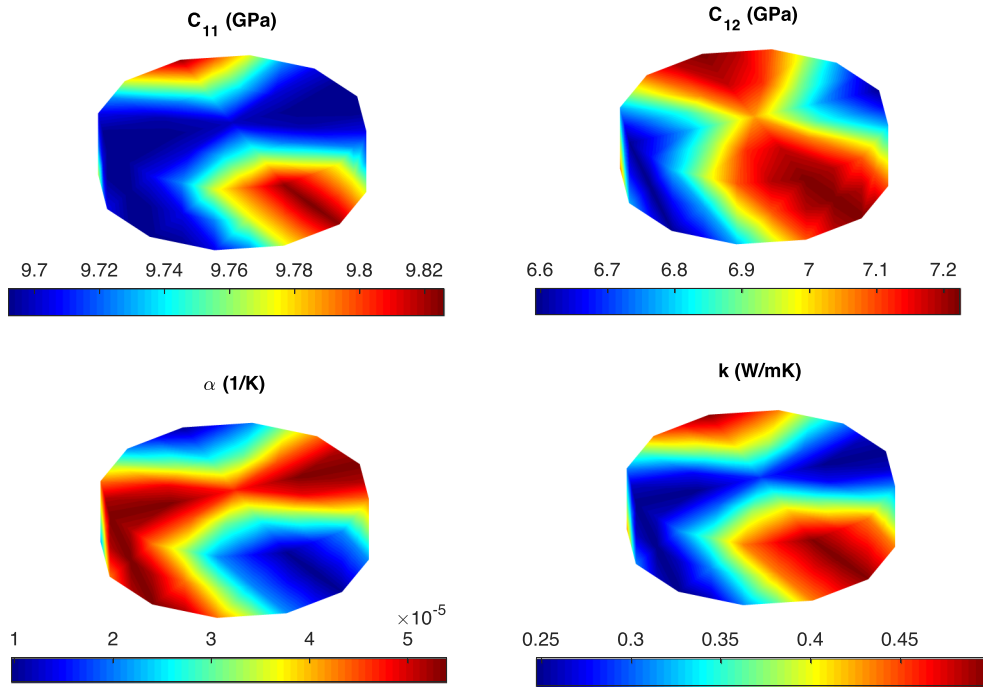


Fig. 4 Single crystal properties for stiffness, thermal expansion and conductivity.

The thermal expansion coefficient of the SWNT can be computed using volume averaging equations that are linear in the ODF. However, the natural frequency design constraints are nonlinear in terms of the design variables (ODF values) as shown in Eqs. (8) and (9):

$$\bar{\omega}_t = \frac{\pi}{2L} \sqrt{\frac{\bar{G}_{12} J}{\rho I_p}} \quad (8)$$

$$\bar{\omega}_b = (\beta L)^2 \sqrt{\frac{\bar{E}_1 I_1}{m L^4}} \quad \text{and} \quad \beta L = 1.87510 \quad (9)$$

where $\bar{G}_{12} = 1/\bar{S}_{66}$, $\bar{E}_1 = 1/\bar{S}_{11}$, and \bar{S}_{11} and \bar{S}_{66} are the compliance elements. In these formulations, J is torsion constant, ρ is density, I_p is polar inertia moment, m is unit mass, L is length of the beam, and I_1 is moment of inertia along axis 1. To solve the problem, the length of the beam is taken as $L = 0.45$ m and the beam is considered to have a rectangular cross section with dimensions $a = 20$ mm and $b = 3$ mm. The formulation of the first bending and torsion natural frequencies as well as the geometric aspects of the same cantilever beam problem for a Galfenol material have been also recently discussed in our earlier works [40,41]. Because of the nonlinear nature of the vibration tuning design constraints, the optimization is solved by implementing the sequential quadratic programming solver to the multiscale design framework of the SWNT. The mathematical representation of the optimization problem is given below:

$$\min \bar{\alpha} \quad (10)$$

$$\text{subject to: } 3 \text{ Hz} \leq \bar{\omega}_t \leq 4 \text{ Hz} \quad (11)$$

$$10 \text{ Hz} \leq \bar{\omega}_b \leq 11 \text{ Hz} \quad (12)$$

$$\mathbf{q}^T \mathbf{A} = 1 \quad (13)$$

Table 1 Optimization results for the LP problem

	\bar{C}_{11} (GPa)	\bar{C}_{12} (GPa)	$\bar{\alpha}$ (1/K)	\bar{k} (W/mK)
Random design	9.7231	6.9760	3.8781×10^{-5}	0.3333
Optimum design	9.8259	7.2237	9.7176×10^{-6}	0.4991

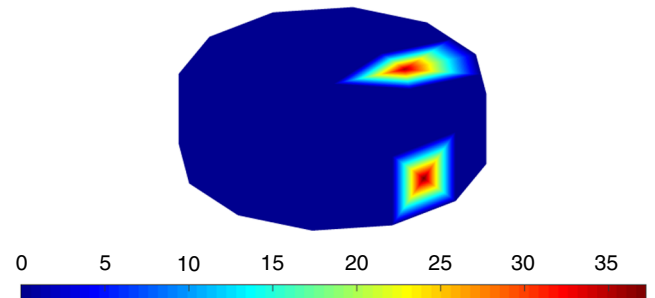


Fig. 5 Optimum ODF representation for nanocomposite.

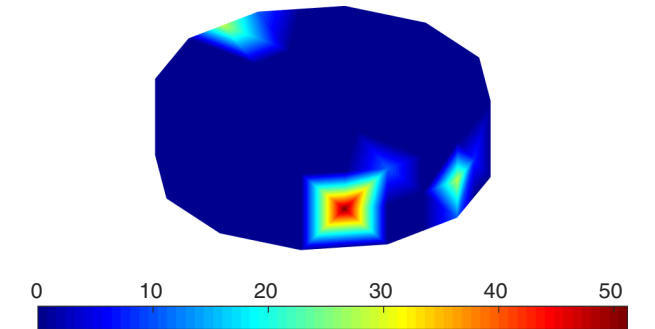


Fig. 6 Optimum ODF solution of the thermal expansion and vibration tuning problem.

$$s = (A_i), \quad \text{where } i = 1, 2, \dots, 50 \quad (14)$$

The optimum ODF solution of the problem is identified as a polycrystal. The optimum design is shown in Rodrigues space in Fig. 6. The optimum design criteria are shown and compared with the random alignment design in Table 2.

Table 2 Optimization results for the thermal expansion and vibration tuning problem

	$\bar{\alpha}$ (1/K)	$\bar{\omega}_t$ (Hz)	$\bar{\omega}_b$ (Hz)
Random design	3.8781×10^{-5}	3.2351	10.3008
Optimum design	1.7796×10^{-5}	3.3950	10.6087

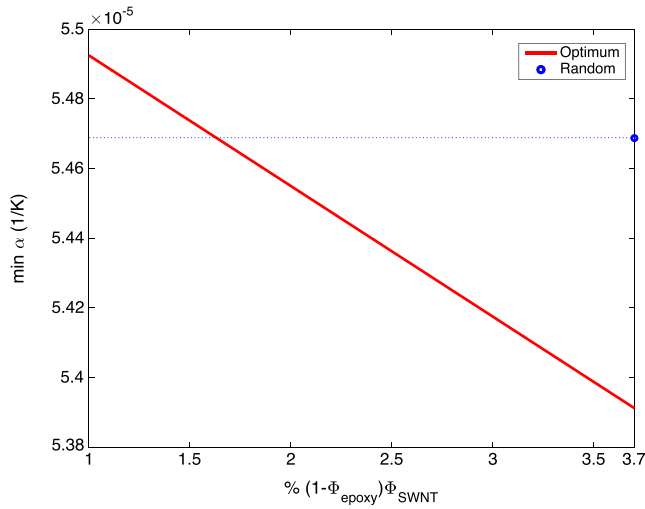


Fig. 7 Variation of the thermal expansion coefficient with respect to SWNT volume fraction.

The automated multiscale optimization methodology provides a very considerable improvement on the thermal and mechanical performance (54.11% decrease for minimum design objective) of the SWNT as indicated by Table 2. This multiscale design framework is powerful because it can easily be implemented to any macro-level engineering application. Another important result here is that the optimization can achieve a design that performs better than the random design even with a lower SWNT volume fraction. The averaged material property values of the nanocomposite can be calculated using volume averaging relations [44]. The following equation shows the example computation for the averaged thermal expansion coefficient, α , of the nanocomposite:

$$\alpha = \bar{\alpha} \times (1 - \Phi_{\text{epoxy}}) + \bar{\alpha}_{\text{epoxy}} \times \Phi_{\text{epoxy}} \quad (15)$$

where $\bar{\alpha}$ is the thermal expansion coefficient of the SWNT that is optimized in this example application, $\bar{\alpha}_{\text{epoxy}}$ is the thermal expansion coefficient of the epoxy (where $\bar{\alpha}_{\text{epoxy}} = 5.53 \times 10^{-5}$ [1/K]), and Φ_{epoxy} is the epoxy volume fraction. Figure 7 shows the change in minimum thermal expansion coefficient of the optimum nanocomposite design with respect to the SWNT volume fraction (Φ_{SWNT}) in comparison with the randomly oriented design.

As indicated by Fig. 7 the optimized nanocomposite design still achieves a more desirable thermal expansion coefficient even with lower SWNT volume fraction values compared with the fixed volume fraction value (3.7%) used in the randomly oriented design. Having a lower SWNT volume fraction is advantageous because it provides a considerable cost reduction. The final nanocomposite design with the optimized SWNT orientations still offers a better solution compared with the random design when SWNT volume fraction is as low as 2%.

VI. Conclusions

This paper outlines a new multiscale modeling and optimization approach for epoxy-SWNT nanocomposites. SWNT alignment in a composite is modeled using a compact representation of the orientation space with a one-point probability descriptor, orientation distribution function (ODF). The ODF representation captures the volume density of different SWNT orientations. The averaged material property values are computed using the volume averaging equations that are linear in terms of the ODF values. The optimal SWNT alignments are identified for two different engineering applications. In the first application, the optimum ODF values representing the optimal SWNT alignment are identified by implementing an optimization methodology based on linear programming (LP). The objective of the optimization problem is to maximize the averaged value of the SWNT stiffness parameter, \bar{C}_{11} . Additional design constraints are defined to improve the other parameters, such as the stiffness elements, thermal conductivity, and thermal expansion, compared with randomly oriented nanotube

alignment. In the next application, a thermal expansion and vibration tuning problem for a cantilever beam is considered. The objective of the optimization is to find the optimum ODFs that minimize the thermal expansion of the beam. The design constraints are defined for the first bending and torsion natural frequencies of the beam for vibration tuning. Because of the nonlinear nature of the constraints, the sequential quadratic programming is implemented to the multiscale modeling environment. The optimum designs of both applications provide very considerable improvement on thermal and mechanical properties of the SWNT. Future work in this area will focus on analyzing the effect of uncertainties to the multiscale design environment developed for SWNTs. Another important future topic would be the investigation of the manufacturing routes of the optimized SWNT solutions. New technology manufacturing techniques using electric and magnetic fields will be studied to improve the variability of designs that can be processed and thus increase the probability for manufacturability.

Acknowledgments

The work presented here was supported by the Defense Threat Reduction Agency HDTRA1-13-1-0009. The authors acknowledge the support of the University of Michigan Center for Advanced Computing (CAC), a high-performance computing center located in the Ann Arbor campus.

References

- [1] Treacy, M. J., Ebbesen, T., and Gibson, J., "Exceptionally High Young's Modulus Observed for Individual Carbon Nanotubes," *Nature*, Vol. 381, No. 6584, 1996, pp. 678–680. doi:10.1038/381678a0
- [2] Yakobson, B. I., and Avouris, P., "Mechanical Properties of Carbon Nanotubes," *Carbon Nanotubes*, Springer, Berlin, 2001, pp. 287–327. doi:10.1007/3-540-39947-X_12
- [3] Walters, D., Ericson, L., Casavant, M., Liu, J., Colbert, D., Smith, K., and Smalley, R., "Elastic Strain of Freely Suspended Single-Wall Carbon Nanotube Ropes," *Applied Physics Letters*, Vol. 74, No. 25, 1999, pp. 3803–3805. doi:10.1063/1.124185
- [4] Thess, A., Lee, R., Nikolaev, P., and Dai, H., "Crystalline Ropes of Metallic Carbon Nanotubes," *Science*, Vol. 273, No. 5274, 1996, pp. 483–487. doi:10.1126/science.273.5274.483
- [5] Wilder, J. W., Venema, L. C., Rinzler, A. G., Smalley, R. E., and Dekker, C., "Electronic Structure of Atomically Resolved Carbon Nanotubes," *Nature*, Vol. 391, No. 6662, 1998, pp. 59–62. doi:10.1038/34139
- [6] Odom, T. W., Huang, J.-L., Kim, P., and Lieber, C. M., "Atomic Structure and Electronic Properties of Single-Walled Carbon Nanotubes," *Nature*, Vol. 391, No. 6662, 1998, pp. 62–64. doi:10.1038/34145
- [7] Dresselhaus, M., and Eklund, P., "Phonons in Carbon Nanotubes," *Advances in Physics*, Vol. 49, No. 6, 2000, pp. 705–814. doi:10.1080/000187300413184
- [8] Hone, J., "Phonons and Thermal Properties of Carbon Nanotubes," *Carbon Nanotubes*, Springer, Berlin, 2001, pp. 273–286. doi:10.1007/3-540-39947-X_11
- [9] Yu, M.-F., Files, B. S., Arepalli, S., and Ruoff, R. S., "Tensile Loading of Ropes of Single Wall Carbon Nanotubes and Their Mechanical Properties," *Physical Review Letters*, Vol. 84, No. 24, 2000, pp. 5552–5555. doi:10.1103/PhysRevLett.84.5552
- [10] Fasanella, N. A., and Sundararaghavan, V., "Molecular Dynamics of SWNT/Epoxy Nanocomposites," *56th AIAA/ASCE/AHS/ASC Structures, Structural Dynamics, and Materials Conference*, AIAA Paper 2015-0124, Jan. 2015. doi:10.2514/6.2015-0124
- [11] Fasanella, N. A., and Sundararaghavan, V., "Atomistic Modeling of Thermomechanical Properties of SWNT/Epoxy Nanocomposites," *Modelling and Simulation in Materials Science and Engineering*, Vol. 23, No. 6, 2015, Paper 065003. doi:10.1088/0965-0393/23/6/065003
- [12] Zhigilei, L. V., "MSE 4270/6270: Introduction to Atomistic Simulations," Lecture Notes, Dept. of Materials Science and Engineering, Univ. of Virginia, 2016.

- [13] Liu, A., Wang, K., and Bakis, C. E., "Effect of Functionalization of Single-Wall Carbon Nanotubes (SWNTs) on the Damping Characteristics of SWNT-Based Epoxy Composites via Multiscale Analysis," *Composites Part A: Applied Science and Manufacturing*, Vol. 42, No. 11, 2011, pp. 1748–1755.
doi:10.1016/j.compositesa.2011.07.030
- [14] Seidel, G. D., and Lagoudas, D. C., "Micromechanical Analysis of the Effective Elastic Properties of Carbon Nanotube Reinforced Composites," *Mechanics of Materials*, Vol. 38, No. 8, 2006, pp. 884–907.
doi:10.1016/j.mechmat.2005.06.029
- [15] Li, C., and Chou, T.-W., "Multiscale Modeling of Carbon Nanotube Reinforced Polymer Composites," *Journal of Nanoscience and Nanotechnology*, Vol. 3, No. 5, 2003, pp. 423–430.
doi:10.1166/jnn.2003.233
- [16] Li, C., and Chou, T.-W., "Multiscale Modeling of Compressive Behavior of Carbon Nanotube/Polymer Composites," *Composites Science and Technology*, Vol. 66, No. 14, 2006, pp. 2409–2414.
doi:10.1016/j.compscitech.2006.01.013
- [17] Namilaie, S., and Chandra, N., "Multiscale Model to Study the Effect of Interfaces in Carbon Nanotube-Based Composites," *Journal of Engineering Materials and Technology*, Vol. 127, No. 2, 2005, pp. 222–232.
doi:10.1115/1.1857940
- [18] Spanos, P., and Kotsos, A., "A Multiscale Monte Carlo Finite Element Method for Determining Mechanical Properties of Polymer Nanocomposites," *Probabilistic Engineering Mechanics*, Vol. 23, No. 4, 2008, pp. 456–470.
doi:10.1016/j.probenmech.2007.09.002
- [19] Tserpes, K., Papanikos, P., Labeas, G., and Pantelakis, S. G., "Multi-Scale Modeling of Tensile Behavior of Carbon Nanotube-Reinforced Composites," *Theoretical and Applied Fracture Mechanics*, Vol. 49, No. 1, 2008, pp. 51–60.
doi:10.1016/j.tafmec.2007.10.004
- [20] Ionita, M., "Multiscale Molecular Modeling of SWCNTs/Epoxy Resin Composites Mechanical Behaviour," *Composites Part B: Engineering*, Vol. 43, No. 8, 2012, pp. 3491–3496.
doi:10.1016/j.compositesb.2011.12.008
- [21] Yang, S., Yu, S., Kyoung, W., Han, D.-S., and Cho, M., "Multiscale Modeling of Size-Dependent Elastic Properties of Carbon Nanotube/Polymer Nanocomposites with Interfacial Imperfections," *Polymer*, Vol. 53, No. 2, 2012, pp. 623–633.
doi:10.1016/j.polymer.2011.11.052
- [22] Yang, S., Yu, S., Ryu, J., Cho, J.-M., Kyoung, W., Han, D.-S., and Cho, M., "Nonlinear Multiscale Modeling Approach to Characterize Elastoplastic Behavior of CNT/Polymer Nanocomposites Considering the Interphase and Interfacial Imperfection," *International Journal of Plasticity*, Vol. 41, Feb. 2013, pp. 124–146.
doi:10.1016/j.ijplas.2012.09.010
- [23] Wang, Y., Maspoch, D., Zou, S., Schatz, G. C., Smalley, R. E., and Mirkin, C. A., "Controlling the Shape, Orientation, and Linkage of Carbon Nanotube Features with Nano Affinity Templates," *Proceedings of the National Academy of Sciences of the United States of America*, Vol. 103, No. 7, 2006, pp. 2026–2031.
doi:10.1073/pnas.0511022103
- [24] TermeshYousefi, A., and Kadri, N. A., "Morphology Optimization of Highly Oriented Carbon Nanotubes for Bioengineering Applications," *Materials Research Innovations*, Vol. 20, No. 4, 2016, pp. 268–271.
doi:10.1080/14328917.2015.1105574
- [25] Wal, R. L. V., Hall, L. J., and Berger, G. M., "Optimization of Flame Synthesis for Carbon Nanotubes Using Supported Catalyst," *The Journal of Physical Chemistry B*, Vol. 106, No. 51, 2002, pp. 13122–13132.
doi:10.1021/jp020614l
- [26] Huang, C., Wang, R. K., Wong, B. M., McGee, D. J., Leonard, F., Kim, Y. J., Johnson, K. F., Arnold, M. S., Eriksson, M. A., and Gopalan, P., "Spectroscopic Properties of Nanotube-Chromophore Hybrids," *ACS Nano*, Vol. 5, No. 10, 2011, pp. 7767–7774.
doi:10.1021/nn202725g
- [27] Wang, Q., Storm, B. K., and Houmiller, L. P., "Study of the Isothermal Curing of an Epoxy Prepreg by Near-Infrared Spectroscopy," *Journal of Applied Polymer Science*, Vol. 87, No. 14, 2003, pp. 2295–2305.
doi:10.1002/app.v87:14
- [28] Knox, C., Andzelm, J., Lenhart, J., Browning, A., and Christensen, S., "High Strain Rate Mechanical Behavior of Epoxy Networks from Molecular Dynamics Simulations," *Proceedings of 27th Army Science Conference*, Orlando, FL, GP-09, 2010.
- [29] Christensen, S., "Atomistically Explicit Molecular Dynamics Simulations of Thermosetting Polymers," *Proceedings of 39th ISTC SAMPE Conference*, Soc. for the Advancement of Material and Process Engineering, Covina, CA, 2007.
- [30] Studio, D., and Insight, I., *Materials Studio User's Manual*, Vol. 92121, Accelrys Software Inc., San Diego, CA, 2009.
- [31] Dauber-Osguthorpe, P., Roberts, V. A., Osguthorpe, D. J., Wol, J., Genest, M., and Hagler, A. T., "Structure and Energetics of Ligand Binding to Proteins: Escherichia Coli Dihydrofolate Reductase-Trimethoprim, a Drug-Receptor System," *Proteins: Structure, Function, and Bioinformatics*, Vol. 4, No. 1, 1988, pp. 31–47.
doi:10.1002/(ISSN)1097-0134
- [32] Plimpton, S., "Fast Parallel Algorithms for Short-Range Molecular Dynamics," *Journal of Computational Physics*, Vol. 117, No. 1, 1995, pp. 1–19.
doi:10.1006/jcph.1995.1039
- [33] Varshney, V., Patnaik, S. S., Roy, A. K., and Farmer, B. L., "Heat Transport in Epoxy Networks: A Molecular Dynamics Study," *Polymer*, Vol. 50, No. 14, 2009, pp. 3378–3385.
doi:10.1016/j.polymer.2009.05.027
- [34] Kumar, A., Sundararaghavan, V., and Browning, A., "Study of Temperature Dependence of Thermal Conductivity in Cross-Linked Epoxies Using Molecular Dynamics Simulations with Long Range Interactions," *Modelling and Simulation in Materials Science and Engineering*, Vol. 22, No. 2, 2014, Paper 025013.
doi:10.1088/0965-0393/22/2/025013
- [35] Fasanella, N. A., and Sundararaghavan, V., "Atomistic Modeling of Thermal Conductivity of Epoxy Nanotube Composites," *Journal of The Minerals, Metals & Materials Society*, Vol. 68, No. 5, 2016, pp. 1396–1410.
doi:10.1007/s11837-016-1861-x
- [36] Bunge, H.-J., *Texture Analysis in Materials Science: Mathematical Methods*, Elsevier, Butterworths, London, 2013, pp. 3–41.
- [37] Sundararaghavan, V., and Zabarar, N., "Linear Analysis of Texture-Property Relationships Using Process-Based Representations of Rodrigues Space," *Acta Materialia*, Vol. 55, No. 5, 2007, pp. 1573–1587.
doi:10.1016/j.actamat.2006.10.019
- [38] Sundararaghavan, V., and Zabarar, N., "On the Synergy Between Texture Classification and Deformation Process Sequence Selection for the Control of Texture-Dependent Properties," *Acta Materialia*, Vol. 53, No. 4, 2005, pp. 1015–1027.
doi:10.1016/j.actamat.2004.11.001
- [39] Kumar, A., and Dawson, P., "Computational Modeling of FCC Deformation Textures over Rodrigues' Space," *Acta Materialia*, Vol. 48, No. 10, 2000, pp. 2719–2736.
doi:10.1016/S1359-6454(00)00044-6
- [40] Acar, P., and Sundararaghavan, V., "Utilization of a Linear Solver for Multiscale Design and Optimization of Microstructures in an Airframe Panel Buckling Problem," *57th AIAA/ASCE/AHS/ASC Structures, Structural Dynamics, and Materials Conference, AIAA SciTech Forum*, AIAA Paper 2016-0156, 2016.
doi:10.2514/6.2016-0156
- [41] Acar, P., and Sundararaghavan, V., "Utilization of a Linear Solver for Multiscale Design and Optimization of Microstructures," *AIAA Journal*, Vol. 54, No. 5, 2016, pp. 1751–1759.
doi:10.2514/1.J054822
- [42] Jones, R. M., *Mechanics of Composite Materials*, CRC Press, Philadelphia, PA, 1998, pp. 480–495.
- [43] Daniel, I. M., Ishai, O., and Daniel, I., *Engineering Mechanics of Composite Materials*, Vol. 3, Oxford Univ. Press, New York, 1994, Chap. 8.
- [44] Schapery, R. A., "Thermal Expansion Coefficients of Composite Materials Based on Energy Principles," *Journal of Composite Materials*, Vol. 2, No. 3, 1968, pp. 380–404.
doi:10.1177/002199836800200308